Open Archive TOULOUSE Archive Ouverte (OATAO)

OATAO is an open access repository that collects the work of Toulouse researchers and makes it freely available over the web where possible.

This is an author-deposited version published in : http://oatao.univ-toulouse.fr/
Eprints ID : 15830

Any correspondence concerning this service should be sent to the repository administrator: staff-oatao@listes-diff.inp-toulouse.fr

Spatio-temporal analysis of factors controlling nitrate dynamics and potential denitrification hot spots and hot moments in groundwater of an alluvial floodplain

Léonard Bernard-Jannin *, Xiaoling Sun, Samuel Teissier, Sabine Sauvage, José-Miguel Sánchez-Pérez *

ECOLAB, Université de Toulouse, CNRS, INPT, UPS, France

ABSTRACT

Nitrate (NO_3^-) contamination of freshwater systems is a global concern. In alluvial floodplains, riparian areas have been proven to be efficient in nitrate removal. In this study, a large spatio-temporal dataset collected during one year at monthly time steps within a meander area of the Garonne floodplain (France) was analysed in order to improve the understanding of nitrate dynamic and denitrification process in floodplain areas. The results showed that groundwater NO_3^- concentrations (mean 50 mg NO_3^- L^{-1}) were primarily controlled by groundwater dilution with river water (explaining 54% of NO_3^- variance), but also by nitrate removal process identified as denitrification (explaining 14% of NO_3^- variance). Dilution was controlled by hydrological flow paths and residence time linked to river-aquifer exchanges and flood occurrence, while potential denitrification (DEA) was controlled by oxygen, high dissolved organic carbon (DOC) and organic matter content in the sediment (31% of DEA variance). DOC can originate both from the river input and the degradation of organic matter (OM) located in topsoil and sediments of the alluvial plain. In addition, river bank geomorphology appeared to be a key element explaining potential denitrification hot spot locations. Low bankfull height (LBH) areas corresponding to wetlands exhibited higher denitrification rates than high bankfull height (HBH) areas less often flooded. Hydrology determined the timing of denitrification hot moments occurring after flood events. These findings underline the importance of integrating dynamic water interactions between river and aquifer, geomorphology, and dual carbon source (river and sediment) when assessing nitrate dynamics and denitrification patterns in floodplain environments.

1. Introduction

Nitrate contamination of groundwater through point source and diffuse pollution has long attracted world-wide attention (Power and Schepers, 1989; Bijay-Singh et al., 1995; Zhang et al., 1996; Arrate et al., 1997; Carpenter et al., 1998; Jégo et al., 2012). Nitrate pollution from agricultural sources is considered to be the main cause of groundwater degradation in the European Union (Sutton et al., 2011). In Europe and North America, up to 90% of floodplain areas are cultivated (Tockner and Stanford, 2002). Agricultural land use, in combination with factors such as shallow groundwater, high permeability of alluvial deposits and interconnections with surface water, make alluvial aquifers particularly vulnerable to nitrate diffuse pollution (Arauzo et al., 2011). As a result, nitrate concentrations exceeding the limit of 50 mg-NO_3^- L^{-1} set for groundwater systems in Europe by the Nitrate Directive (91/676/EEC) and the Groundwater Directive (2006/118/EEC) have been reported for several shallow aquifers in floodplain areas (Baillieux et al., 2014; Sánchez-Pérez et al., 2003).

Floodplain environments are characterised by strong surface water-groundwater interactions that are important for aquifer water composition (Amoros et al., 2002; Sun et al., 2015). Nitrate contamination in shallow aquifers can therefore be mitigated by the dilution resulting from mixing with river water containing low nitrate concentrations (Pinay et al., 1998; Baillieux et al., 2014). Nitrate mass removal also occurs through natural biogeochemical processes such as plant uptake, denitrification, dissimilatory nitrate reduction to ammonium and microbial immobilisation,

among which denitrification is reported to be the most important in groundwater (Korom, 1992; Burt et al., 1999; Rivett et al., 2008).

Denitrification is the anaerobic reduction of nitrate (NO_3^-) into gaseous compounds (nitrous oxide or dinitrogen) by microorganisms. Denitrification in groundwater is linked to: (i) presence of nitrate, denitrifying bacteria and organic carbon (OC) as electron donor, (ii) anaerobic conditions and (iii) favourable environmental conditions in terms of e.g. temperature and pH (Rivett et al., 2008). However, among all these factors, availability of OC has been identified as the major limiting factor in nitrate-contaminated groundwater (see Rivett et al. (2008) for a review).

Riparian zones are located at the interface between aquatic and terrestrial environments (Vidon et al., 2010). In these areas, where surface water rich in organic matter (OM) meets groundwater containing abundant nutrients, denitrification is promoted (Hill et al., 2000; Sánchez-Pérez et al., 2003). Therefore riparian areas have been shown to be efficient in nitrate pollution mitigation (Vidon and Hill, 2006; Dosskey et al., 2010; Naiman et al., 2010). In these systems, the hydrological exchanges at the river/groundwater interface can have a significant impact on denitrification rates in the aquifer (Baker and Vervier, 2004; Lamontagne et al., 2005). Such exchanges recharge aquifer with river water rich in OM, stimulating denitrification in groundwater (Iribar, 2007; Sánchez-Pérez et al., 2003). The location of the denitrification process is driven by advective flux, where flow paths lead organic matter and nitrate to meet (Seitzinger et al., 2006), at points defined as hot spots by McClain et al. (2003). At the scale of the floodplain section, denitrification is usually triggered by NO_3^- input from upland areas and hot spots can be located at the interface between the upland and riparian zones, between the riparian zone and the stream or within the riparian zone (McClain et al., 2003). At this scale, the efficiency of the riparian area in nitrate removal is reported to be related to hydrogeomorphic characteristics associated with geological and hydrological settings (Groffman et al., 2009), such as water residence time (Seitzinger et al., 2006). In addition, the occurrence of hot spots may vary in time, especially in environments with strong temporal variations in hydrological conditions. For example, denitrification rates have been found to be higher in high flow conditions (Baker and Vervier, 2004; Iribar, 2007; Peter et al., 2011), within periods corresponding to hot moments (McClain et al., 2003). Therefore, studies on denitrification processes need to take into account both spatial and temporal scale with suitable resolution in order to accurately describe the processes at stake and their impact on nitrate dynamics.

The main objective of this study was to examine the occurrence of potential denitrification hot spots and hot moments and their relationship to environmental conditions, in order to improve knowledge on nitrate dynamics in floodplains. Based on a high spatial resolution dataset collected during 12 monthly sampling campaigns, we sought to: (i) identify the factors best explaining nitrate concentrations variations and explored their spatio-temporal patterns; (ii) identify the factors best explaining potential denitrification rates measured in aquifer sediment samples; and (iii) analyse the occurrence of denitrification hot spots/hot moments according to the controlling factors in order to develop a conceptual diagram of denitrification process in floodplain environments.

2. Materials and methods

2.1. Study site

The study area, which covers about 50 ha, is located within a 2 km long meander in the middle section of the Garonne river watershed, close to the village of Monbéqui in south-west France (Fig. 1). Mean annual precipitation in the area is 660 mm. The drainage area of the Garonne watershed at the study site is about 13,730 km^2, with annual average flow of 190 m^3 s^{-1} and a range from 98 m^3 s^{-1} (1989) to 315 m^3 s^{-1} (1978) over the past 41 years. The driest month is August, with 76 m^3 s^{-1} on average, and the wettest is May, with 343 m^3 s^{-1} on average. The daily flow is highly variable, ranging from 10 m^3 s^{-1} during the severe drought in August 1991 to 2930 m^3 s^{-1} during the largest flood event recorded, on 6 November 2000 (www.hydro.eaufrance. fr). The two-year return period flood corresponds to daily flow of 1400 m^3 s^{-1}. The floodplain comprises 4–7 m of quaternary sand and gravel deposits (mean saturated hydraulic conductivity 10^{-3} m s^{-1}), overlying impermeable molassic bedrock. In this area the Garonne River fully penetrates the alluvial formation, so that the riverbed lies on the impermeable substratum. The alluvial deposits are covered with a silty soil layer 1–2 m deep and containing 1.5% OM on average (Jégo et al., 2012). The connection between aquifer and the Garonne river is strongly influenced by hydrological conditions (Sun et al., 2015). The floodplain is heavily cultivated (irrigated maize, sunflower, sorghum, wheat), leading to major nitrate influx into the groundwater. Concentrations of 100 mg-NO_3^- L^{-1} are common (Sánchez-Pérez et al., 2003). A small area of riparian forest, mainly composed of willow (Salix alba) and ash trees (Fraxinus excelsior), is located close to the river at a lower elevation than the rest of the study area, and is separated from the agricultural fields by plantations of poplar (Populus alba) (Fig. 1). The geomorphology of the river bank on the right side of the river can be separated into two types: Low bankfull height type (LBH) corresponding to the profile A–A′ (Fig. 1), which is regularly flooded as the groundwater level is often close to the surface and can be designated as permanent wetland; and high bankfull height type (HBF), corresponding to the profile B–B′, which is only flooded during the highest floods (greater than two-year return period flood events). Three piezometers (P6, P9 and P13) are located within a LBH area.

Previous studies carried out on this area have demonstrated the role of DOC borne by the river into the aquifer in denitrification (Sánchez-Pérez et al., 2003) and the importance of the sediment-attached bacterial community for aquifer denitrification (Iribar et al., 2008). In addition, modelling studies have shown the importance of river-aquifer exchanges for groundwater composition (Weng et al., 2003; Peyrard et al., 2008; Sun et al., 2015) and the impact of agricultural practices on nitrate leaching into the shallow aquifer (Jégo et al., 2012).

2.2. Sampling

A network of 22 piezometers (internal diameter 51 mm, with 1 mm slots) was installed throughout the study site between the Garonne river and the agricultural fields (Fig. 1). Water samples were collected within each piezometer during monthly sampling campaigns from April 2013 to March 2014, providing a high-spatial resolution dataset with around 50–100 m between sampling points. In four of these campaigns, called full campaigns, additional sediment sampling was performed (Fig. 2).

After measuring water table depth (WD), as the distance between soil surface and water table surface, water was pumped with a thermal motor pump and physico-chemical parameters in water were measured once electrical conductivity (EC) had stabilised (Sánchez-Pérez et al., 1991a, 1991b). Dissolved oxygen (DO), temperature (T), pH and EC were measured using a portable metre (WTW Multi 3420) and specific probes. Water samples were then filtered through 0.45 μm cellulose acetate membrane filters. Anion concentrations, i.e. nitrate (NO_3^-), chloride (Cl$^-$), sulphate (SO_4^{2-}) and phosphate (PO_4^{3-}), and cation concentrations, i.e. calcium (Ca^{2+}), magnesium (Mg^{2+}), potassium (K$^+$), sodium (Na$^+$)
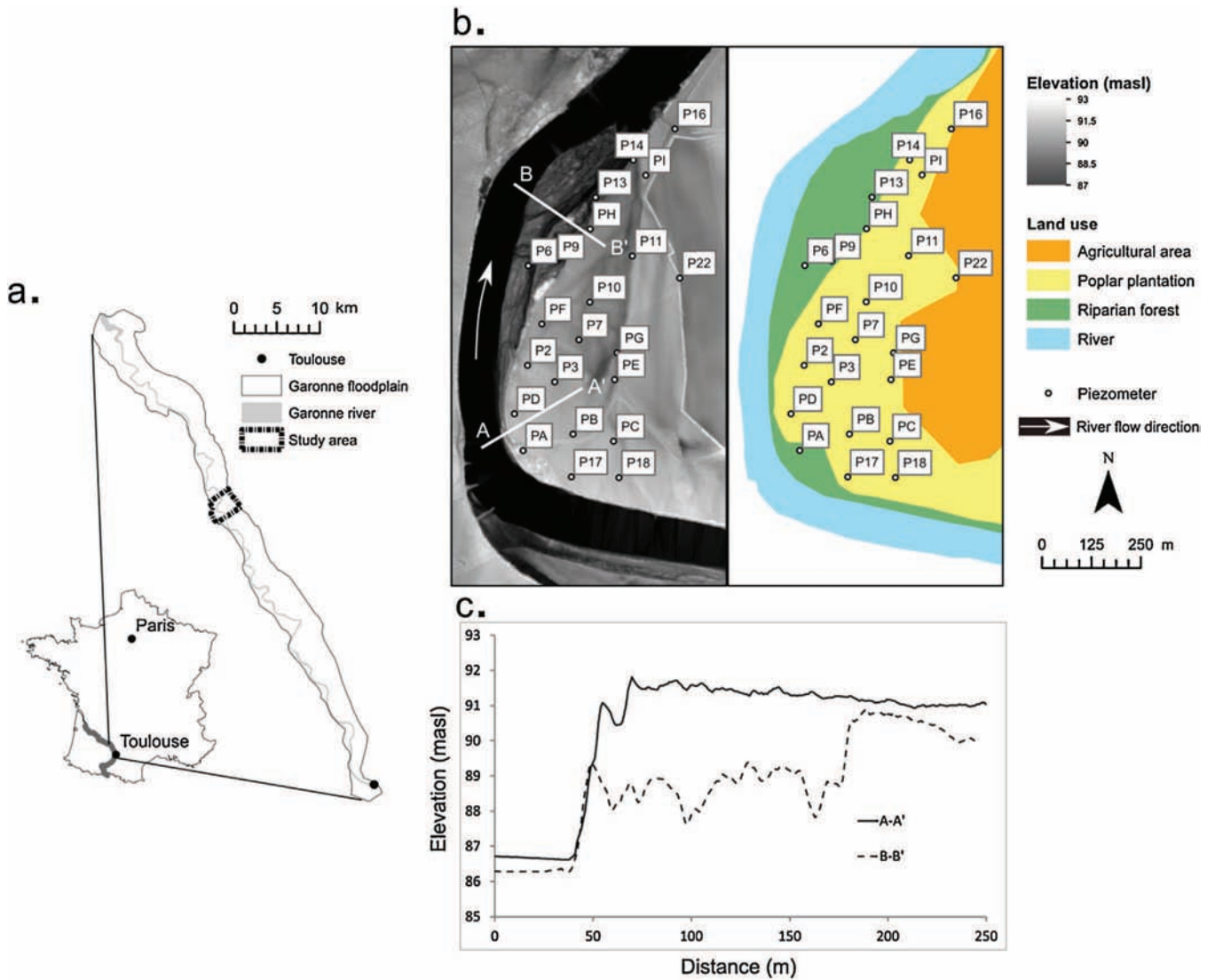
Fig. 1. (a) Geographical location; (b) digital terrain elevation and land use map of the study area, showing the network of piezometers (PA–P22) used in the present study; and (c) vertical profiles at two locations (A–A′ and B–B′).

and ammonium (NH_4^+), were determined by ion chromatography (Dionex ICS-5000+ and DX-120). Silica concentration was determined by spectrophotocolorimetry (Alpkem) and alkalinity (Alk) by acid titration. Water samples collected for determination of DOC concentration were filtered through rinsed 0.45-μm cellulose acetate membrane filters, stored in carbon-free glass tubes, acidified with HCl and combusted using a platinum catalyser (Shimadzu, Model TOC 5000) at 650 °C. For the four full campaigns, sediment was sampled after water sampling by increasing the pumping velocity for 5–10 min, with the water flowing into a 50-L tank where sediments settled before being collected together with 100 mL water in sealed sterile bags. In the river, *in situ* physicochemical measurements (DO, T and pH) were made and water was sampled directly within the stream. All the samples were immediately stored at 4 °C after collection.

Oxygen isotope composition was measured by isotope ratio mass spectrometry after CO_2–H_2O equilibration using the technique described by Epstein and Mayeda (1953). The results were expressed relative to a standard (V-SMOW, Gonfiantini, 1978) using delta notation (δ), where $\delta^{18}O$ is given by:

$$\delta^{18}O = \frac{R^{18}O_{sample} - R^{18}O_{V\text{-SMOW}}}{R^{18}O_{V\text{-SMOW}}}$$

where $R^{18}O_{sample}$ and $R^{18}O_{V\text{-SMOW}}$ are the $^{18}O/^{16}O$ ratios for the sample and V-SMOW, respectively. As the difference between samples and standard is small, the 'δ-value' is usually expressed in parts per 1000 [‰].

2.3. Denitrifying enzyme activity (DEA)

Assessments of denitrifying enzyme activity (DEA) were conducted in the laboratory within the week following sediment sample collection. Each sediment sample was analysed in triplicate. A 25 mL portion of wet sediment and 50 mL deoxygenated milliQ water containing KNO_3^- and sodium acetate, to give final concentrations of 100 mg-N L^{-1} and 50 mg-C L^{-1}, respectively, were added to a gas-tight 150-mL serum bottle. After complete deoxygenation (N_2 sparging), inhibition of N_2O reductases was achieved by injecting 15 mL C_2H_2. Incubations were performed in the dark at 14 °C, corresponding to the average measured temperature of the groundwater in the study area. Atmospheric pressure in the serum bottles was ensured during incubation (removal of gas phase before C_2H_2 addition and addition of N_2 to compensated samples). Gas samples were taken from the gas phase of the serum bottles after vigorous shaking, at 30 min and 6 h 30 min after C_2H_2 injection. N_2O was determined by injection into a Varian CP 3800 gas chromatograph
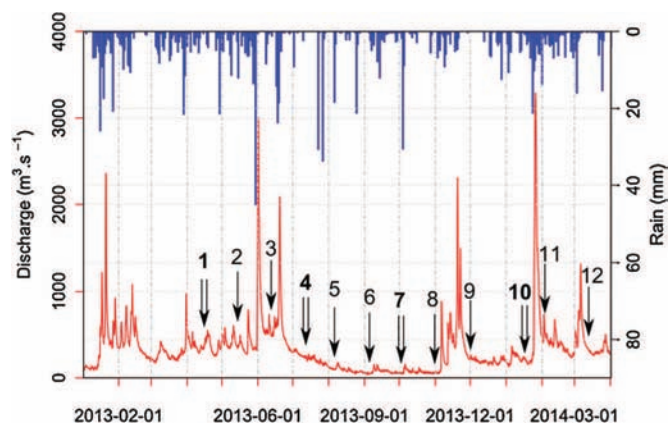
Fig. 2. Water discharge (red) and rain (blue) in the study area. Arrows and numbers indicate sampling periods (simple arrows for regular sampling campaigns and double arrows with bold numbers for full campaigns). (For interpretation of the references to colour in this figure legend, the reader is referred to the web version of this article.)

fitted with an electron capture detector. Calculations were performed with N_2O solubility coefficients taken from Weiss and Price (1980). The DEA results were expressed in μg of N per g of dry sediment per hour [μg-N g-sed^{-1} h^{-1}] by averaging the rates of N_2O production for the triplicate samples. DEA represents the maximum rate of denitrification that can occur when C and N are freely available and was used in this study as a proxy for the denitrification capacity of the different sampling locations at the sampling times.

After incubation, each sediment sample was dried (105 °C, 24 h) and combusted (550 °C, 4 h) in order to determine sediment OM content, which was expressed as a percentage of dry sediment weight.

2.4. Bacterial richness

DNA was extracted after centrifugation of the sediment samples and PCR amplification of 16S rRNA genes was performed. Electrophoresis was used to produce T-RFLP profiles. Bacterial richness (BR) corresponded to the number of T-RF (corresponding to peaks on the T-RFLP pattern and defined hereafter as OTU, Operational Taxonomic Unit) per sample. Presence/absence data were used in the analyses.

2.5. Data analysis

Data treatment involved 20 parameters, including a descriptor of the hydrological conditions (WD), physico-chemical parameters of the groundwater samples (DO, T, pH, DOC, Alk, SiO_2, NO_3^-, Cl^-, SO_4^{2-}, PO_4^{3-}, Ca^{2+}, Mg^{2+}, K^+, Na^+, NH_4^+, $\delta^{18}O$), biological parameters (BR and DEA) and a sediment-related parameter (OM). EC was used to ensure the stability of water characteristics during the sampling, but it was not used in data analysis as it was already represented through the major ions concentration data. Variables were transformed to ensure normality of their distribution when necessary. Partial least squares regression (PLSR), which is a very suitable method for ecological studies analysing a large array of related predictors (Carrascal et al., 2009), was performed here to relate NO_3^- and DEA to the other environmental factors. PLSR is a technique that combines features from principal component analysis and multiple regression to analyse the effects of linear combinations of several predictors *X* on a response variable *Y*. Associations are established with latent factors defined as linear combinations of predictor variables that maximise the explained variance of the dependent variable (Carrascal et al., 2009; Abdi, 2010). One of

the interesting features of PLSR is that the relationships between the predictors and the response function can be inferred from the weights and regression coefficients of individual predictors in the most explanatory components (Yan et al., 2013). Leave-one-out (LOO) cross-validation was performed to select the number of components and jack-knife estimation was used to test the signification of the coefficients (Mevik and Wehrens, 2007). For each PLSR, the percentage of variance explained for the response variable and the cross-validated root mean square error (RMSECV) were calculated. After the pre-analysis of the data, NH_4^+ and PO_4^{3-} were not selected for the statistical method because their concentrations were very low and below the limit of detection for more than, respectively, 25% and 66% of the measurements. PLSR was performed on the 14 parameters available for the 12 campaigns for NO_3^- (WD, DO, T, pH, DOC, Alk, SiO_2, Cl^-, SO_4^{2-}, Ca^{2+}, Mg^{2+}, K^+, Na^+, $\delta^{18}O$) and on the 17 parameters available for the four full campaigns for DEA (WD, DO, T, pH, DOC, Alk, NO_3^-, SiO_2, Cl^-, SO_4^{2-}, Ca^{2+}, Mg^{2+}, K^+, Na^+, $\delta^{18}O$, OM, BR). All statistical analyses were performed using R 3.1.1 software (R Core Team, 2012).

Interpolation of groundwater level, NO_3^-, DEA, DOC, OM, DO and PLSR component score values to produce maps was performed using the Inverse Distance Weight (IDW) method implemented on ArcGis 10.0 (ESRI, 2011).

3. Results

3.1. Hydrology of the study area

In all the sampling campaigns, the groundwater levels indicated groundwater flow from the alluvial plain to the river. Groundwater level for the four full sampling campaigns is shown in Fig. 3. In campaigns 1 and 10, which took place more than 50 days after the last peak flow ($Q > 1400\,m^3\,s^{-1}$) and in relatively high flow conditions, the hydraulic gradient was smaller than for the other two full campaigns. Campaign 4 took place a few days after the largest flood recorded during the study period and the hydraulic gradient was the highest observed. Campaign 7 took place during a low water period, a few months after the same large flood before campaign 4, and the hydraulic gradient was lower (Table 1 and Fig. 3).

For all four campaigns, the main water flow direction was from the centre of the meander to the north-west. However, some water flow to the west and south-west of the meander was detected in campaigns 4, 7 and 10 (Fig. 3). Overall, the hydraulic gradient ranged from 1‰ to 6‰, which represents water flow velocities ranging from 0.09 to 0.52 m day^{-1}, considering a saturated hydraulic conductivity of 10^{-3} m s^{-1}. Depending on the location, the residence time of the water flowing from the agricultural field to the river was estimated to vary from 100 days in the north of the meander (location A, Fig. 3) to 3000 days in the south of the meander (location B, Fig. 3).

Table 1
Hydrological characteristics of the study area during the four full sampling campaigns.

Campaign	Discharge [$m^3\,s^{-1}$]	Time from last peak flow ($Q > 1400\,m^3\,s^{-1}$) [days]	Sampling date
1	337	79	8–10 April 2013
4	314	13	1–3 July 2013
7	53	104	30 September–2 October 2013
10	209	54	13–15 January 2014

Table 2
Characteristic of the 20 parameters measured in the piezometers: mean value, standard deviation (SD) minimum (min), maximum (max) and coefficient of variation (CV). Mean values for the parameters measured in the river are also presented (river mean). n indicates the number of campaign for which the parameter is available.

	Mean	SD	Min	Max	CV	River mean	n
WD [m]	3.19	1.20	0.16	5.67	38%	–	12
DO [mg L^{-1}]	3.45	2.44	0.06	9.69	71%	10.6	12
T [°C]	13.72	1.12	10.70	16.00	8%	13.27	12
pH [–]	6.94	0.14	6.40	7.88	2%	8.01	12
DOC [mg L^{-1}]	1.03	0.65	0.26	4.87	63%	1.65	12
Alk [mg L^{-1}]	6.26	1.16	2.80	9.90	19%	2.26	12
NO$_3^-$ [mg L^{-1}]	49.57	36.29	0.60	139.40	73%	8.06	12
Cl$^-$ [mg L^{-1}]	53.77	29.62	7.57	196.63	55%	9.11	12
SO$_4^{2-}$ [mg L^{-1}]	73.60	35.82	5.70	283.10	49%	19.96	12
SiO$_2$ [mg L^{-1}]	11.79	3.17	4.10	26.70	27%	4.90	12
Ca^{2+} [mg L^{-1}]	132.89	42.12	32.60	231.47	32%	48.66	12
Mg^{2+} [mg L^{-1}]	19.99	7.31	5.00	37.10	37%	4.93	12
K$^+$ [mg L^{-1}]	2.52	0.99	0.77	6.02	39%	1.50	12
Na$^+$ [mg L^{-1}]	24.84	10.32	7.40	65.00	42%	8.06	12
NH$_4^+$ [mg L^{-1}]	0.07	0.28	<d	2.78	368%	0.05	12
PO$_4^{3-}$ [mg L^{-1}]	0.02	0.07	<d	1.16	352%	0.03	12
δ^{18}O [‰]	−8.88	1.02	−11.54	−5.62	12%	−10.81	12
BR [number of OTU]	13.15	6.50	2.00	36.00	49%	–	4
DEA [μg-N g-sed^{-1} h^{-1}]	2.15E−02	3.63E−02	2.42E−04	1.83E−01	169%	–	4
OM [%]	0.55	0.17	0.16	1.05	31%	–	4

3.2. Biogeochemical characteristics of the study area

Mean values of the 20 parameters recorded during the 12 campaigns (four full campaigns for BR, DEA and OM) in the 22 piezometers and average river characteristics are summarised in Table 2. The average WD was typical of a shallow aquifer, 3.19 m on average, and ranged from 5.67 m to almost at the surface (0.16 m). Nitrate concentrations showed great variation, from 0.6 to 139 mg L^{-1} (coefficient of variation (CV) 73%). The Ca^{2+}, SO$_4^{2-}$ and Cl$^-$ concentrations were relatively high (>50 mg L^{-1} on average). The average NH$_4^+$ and PO$_4^{3-}$ concentration were rather low (<0.1 mg L^{-1}), but on occasion reached higher concentrations. Biological and sediment-related parameters also exhibited strong variability. DEA values varied by several orders of magnitude (2.42×10^{-4}–1.83×10^{-1} μg-N g-sed^{-1} h^{-1}, CV = 169%). Bacterial richness and OM were also very variable (CV 49% and 31%,

respectively), while T, pH and δ^{18}O were the parameters with the smallest variability. Overall, DO, NO$_3^-$, DEA, PO$_4^{3-}$ and NH$_4^+$ were the most variable parameters.

3.3. Nitrate dynamic in the floodplain

Nitrate concentration maps showed a clear difference in concentration between north and south of the meander, with the north being highly concentrated and the south showing lower nitrate concentrations (Fig. 4). However, the NO$_3^-$ concentrations were lower in P6 and P13, both located in the low riparian area than in the north-west part of the meander, close to the agricultural fields, in full sampling campaigns 1, 4 and 10. On a temporal scale, NO$_3^-$ concentrations were higher in campaign 7, after a long low water period. In addition, in this campaign some points (PG, PE,
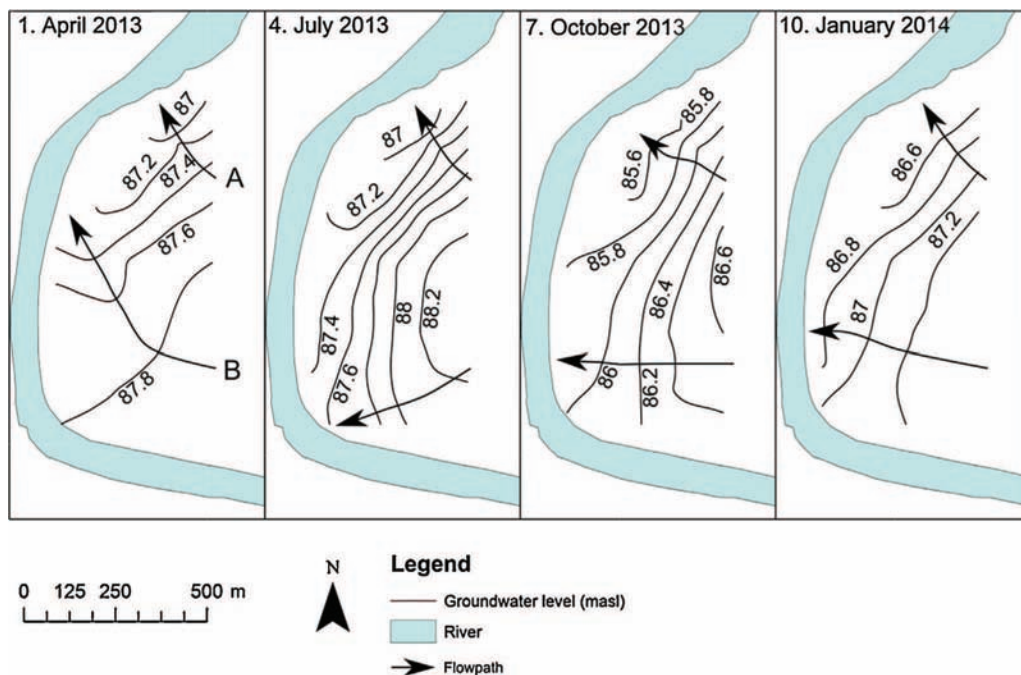
Fig. 3. Groundwater level in the study area and groundwater flowpaths from two locations in the meander (one in the north, A, and one in the south, B) observed in the four full campaigns (1, 4, 7, and 10).
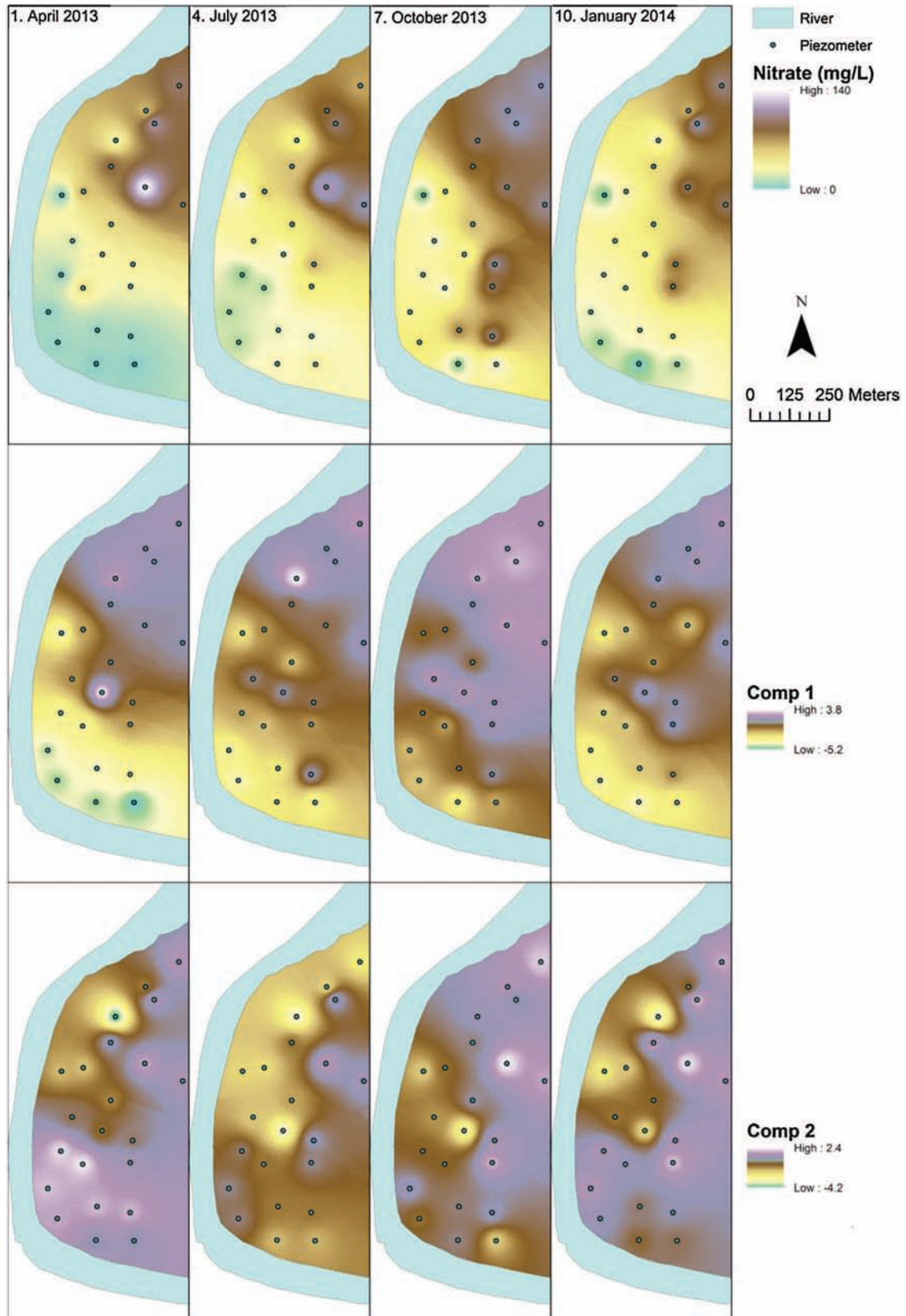
Fig. 4. Maps of interpolated (IDW) nitrate concentrations and of the scores of the first (comp1) and second components (comp2) of the PLSR performed on NO_3^- for the four full sampling campaigns.

Table 3

Summary of the PLSR analysis on NO_3^-. RMSECV is the root mean square error of the cross-validation.

Component	Cumulative % of explained variability in NO_3^-	% of explained variability in NO_3^-	RMSECV
1	56.44	56.44	0.668
2	70.82	14.38	0.545
3	72.65	1.83	0.543
4	74.19	1.54	0.537
5	75.90	1.71	0.525

Table 4

Results of the PLSR on NO_3^- with 14 predictors available for the 12 sampling campaigns. p-Values are based on jack-knife estimates. W1 and W2 are the loadings weight of each predictor on components 1 and 2 (values >0.3 are shown in bold and values <0.1 are not shown).

	Estimate	p value	W1	W2
Mg^{2+}	0.16	<2.20E−16	**0.402**	
$\delta^{18}O$	0.25	<2.20E−16	**0.418**	0.288
Cl^-	0.16	<2.20E−16	**0.398**	
DO	0.23	1.91E−15	0.272	**0.458**
DOC	−0.15	4.27E−14	−0.113	**−0.407**
Na^+	0.06	6.72E−06	**0.304**	−0.268
K^+	0.10	9.66E−06	0.29	
T	0.10	4.20E−05	0.158	0.113
Alk	−0.09	1.94E−05		**−0.427**
SiO_2	0.09	1.02E−04	0.253	
SO_4^{2-}	0.05	3.95E−03	0.292	−0.257
pH	0.08	6.24E−03		**0.382**
Ca^{2+}	0.06	0.0129	0.248	−0.174
WD	0.03	0.134		0.146

Table 5

Summary of the PLSR analysis on DEA. RMSECV is the root mean square error of the cross-validation.

Component	Cumulative % of explained variability in DEA	% of explained variability in DEA	RMSECV
1	41.32	41.32	0.831
2	45.00	3.68	0.807
3	47.00	2.00	0.826
4	48.06	1.06	0.837
5	48.88	0.82	0.872

Table 6

Results of the PLSR on DEA with 17 predictors available for the four full sampling campaigns. p-Values are based on jack-knife estimate. W1 are the loadings weight of each predictor on component 1 (values >0.3 are shown in bold and values <0.1 are not shown).

	Estimate	p value	W1
DOC	0.20	2.33E−06	**0.494**
DO	−0.20	5.30E−06	**−0.493**
OM	0.20	2.13E−04	**0.489**
Alk	0.10	2.52E−03	0.246
NO_3^-	−0.11	0.018	−0.264
K^+	−0.11	0.036	−0.275
Ca^{2+}	0.06	0.19	0.148
$\delta^{18}O$	−0.05	0.29	−0.119
WD	−0.04	0.35	
Mg^{2+}	−0.04	0.41	
T	−0.03	0.50	
BR	0.03	0.59	
Na^+	0.02	0.67	
SiO_2	0.01	0.79	
Cl^-	−0.01	0.85	
SO_4^{2-}	0.01	0.86	
pH	0.00	0.91	

PC) located close to the agricultural fields exhibited high nitrate concentrations.

The factors explaining the NO_3^- concentration variations within the study area were investigated with a PLSR analysis (Table 3). The two first components were selected, which explained, respectively, 56% and 14% of the variance of NO_3^-. The next component only added 2% of the explained variance and the decrease in RMSECV when using three components was relatively low compared with the RMSEC obtained with two components (<1%).

Overall, the most significant predictors ($p < 0.001$), in decreasing order, were Mg^{2+}, $\delta^{18}O$, Cl^-, DO, DOC, Na^+, K^+, T, Alk and SiO_2 (Table 4). The least significant and only parameter with $p > 0.1$ was WD. The correlation was positive between NO_3^- and the regression coefficients of all the variables except DOC and Alk. The most important predictors contributing to the first component were Mg^{2+}, $\delta^{18}O$, Cl^- and Na^+, which accounted for 59% of the component 1 composition. SO_4^{2-} and K^+ were also important and when considering these variables, the contribution to component 1 rose to 76%. All these variables had a positive weight on the first component. Considering the second component, the most important variables contributing to it were DO and pH (positive contribution) and DOC and Alk (negative contribution). These four variables contributed 70% of component 2. This value rose to 92% when adding $\delta^{18}O$ (positive contribution) and Na^+ and SO_4^{2-} (negative contribution).

The score of each component was positively correlated with NO_3^- and was calculated for each piezometer and for each campaign. The resulting interpolated maps for the four full campaigns are shown in Fig. 4. Component 1 exhibited spatial differences between the north and south of the meander, being higher in the north than in the south. In addition, the component 1 scores were higher in summer after the drying stage phase (campaign 7) and the extent of the north area with high values was greater than for the other campaigns.

The second component also displayed spatial differences but for this component, it was the north-west zone of the meander which had lower scores than the remaining area except for the campaign 7. For that campaign, component 2 had lower scores in the east and for two isolated piezometers in the south. Overall, the component score was lower after the large flood (campaign 4) than for the other sampling campaigns.

3.4. Localisation and factors controlling DEA hot spots and hot moments

The spatial heterogeneity of DEA is clearly apparent from the maps in Fig. 5. High DEA values greater than 0.1 μg-N g-sed^{-1} h^{-1} (corresponding to DEA hot spots) were observed in the LBH area (P6, P9 and P13) in campaigns 1, 4 and 7. In addition, relatively high values (>0.05 μg-N g-sed^{-1} h^{-1}) were observed in the piezometers close to the river in campaign 4 (P3, P10, P14, P17, PD). In campaign 7, DEA remained high in piezometers located in the LBH area (especially P6 and P9). Finally, DEA appeared to be lower during campaign 10 and only P3 had a DEA greater than 0.05 μg-N g-sed^{-1} h^{-1}.

The factors explaining the DEA variations within the study area were investigated with a PLSR analysis. Only the first component was selected and explained 41% of DEA variance (Table 5). The next component only added 4% of the explained variance and the decrease in RMSECV when using two components was relatively low compared with the RMSEC calculated with one component (<4%).

The most significant predictors ($p < 0.001$), in decreasing order, were DOC, DO, and OM (Table 6). DOC and OM were positively correlated with DEA, while DO was negatively correlated with DEA. These three parameters contributed 76% of the composition of the first components. Other parameters relatively important in explaining DEA variance ($p < 0.05$) were Alk (positive correlation), NO_3^- and K^+ (negative correlation). Parameters such as WD, Mg^{2+},
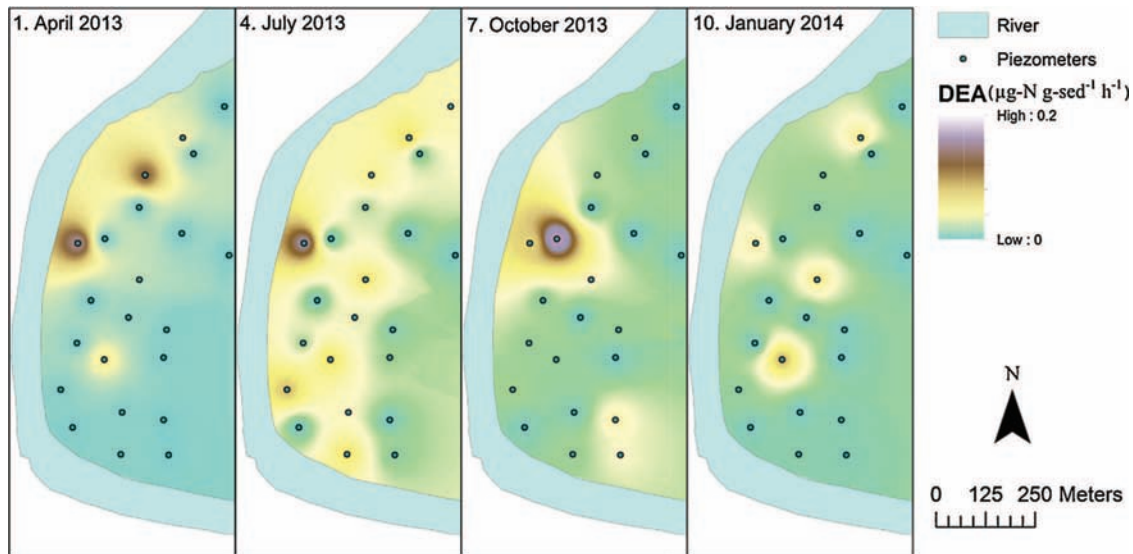
Fig. 5. Maps of interpolated (IDW) denitrifying enzyme activity (DEA) for the four full campaigns.

T, BR, Na$^+$, SiO$_2$, Cl$^-$, SO$_4^{2-}$ and pH were the least important (weight <0.1).

3.5. DOC and OM dynamics in the floodplain

As OC is a key element for the denitrification process, the variability in DOC and OM at the study site was investigated. The DOC maps showed strong temporal variations between sampling campaigns (Fig. 6). The DOC concentrations were the highest over the entire meander in campaign 4, corresponding to the period after the largest flood event recorded during the study period. Spatially, DOC concentrations were rather homogeneous over the meander except for one piezometer where values were higher (P13).

A map of OM content of the sediment is also shown in Fig. 6. In the first campaign, two piezometers exhibited high values (P3 and P11), while the others were relatively low compared with in the other campaigns (especially campaign 4, where OM values were higher than in other campaigns). Overall, OM was rather spatially and temporally homogenous (CV = 31%), but some locations (P3, P7, P11) showed particularly high OM content (>0.8%).

3.6. Bank geomorphology effect on variables controlling denitrification

Bank geomorphology in the study area differed between LBH and HBH areas. Boxplots of variables related to DEA and WD between LBH and HBH are shown in Fig. 7. LBH areas had a greater DEA ($p < 0.01$), a water table closer to the surface, lower DO values and higher DOC values ($p < 0.001$) than HBH areas. However, the OM content was not significantly different between the two bank geomorphology types ($p = 0.31$).

4. Discussion

4.1. Processes controlling spatio-temporal variations in nitrate concentrations at the study site

The PLSR performed on NO$_3^-$ concentrations indicated that the two first components explained 56% and 14% of NO$_3^-$ variance. The first component was mainly related to major ions concentrations, especially Mg^{2+}, Cl$^-$, Na$^+$, but also to high δ^{18}O values. This component can be related to the degree of mixing between the groundwater, characterised by high concentrations of ions (Cl$^-$, SO$_4^{2-}$, Ca^{2+}, Mg^{2+}, Na^{2+}) resulting from agricultural activities and fertiliser input (Böhlke, 2002) and water-aquifer interactions, and the river water, with lower ion concentrations. In addition, δ^{18}O is known to be a good tracer of different water bodies such as surface and subsurface water (Kendall and McDonnell, 2012). Therefore, the first component can be seen as an indicator of the intensity of mixing and of the connectivity between the river and the groundwater, primarily controlling nitrate concentration in the area, with high scores representing high groundwater proportion and low scores high river water proportion. Spatial mapping of the score of the first component for different campaigns indicated that the degree of mixing was linked to the hydrology of the area. According to the groundwater level (Fig. 3), the dominant groundwater flow direction was from the agricultural area north of the meander, and the water in this area therefore had a lower residence time than in the south of the area, where groundwater flow velocities were lower. This is in good agreement with high score of component 1 in the north of the meander and the low score in the south of the meander. Therefore, the influence of the river was greater in the south of the meander, where the flooding occurrence could be higher than the residence time of the groundwater, leading to an area of permanently low ion concentrations. In addition, temporal variations in the degree of mixing between groundwater and river water were observed. The influence of the groundwater affected a greater area in campaign 7, more than three months after the last significant flood event, than for the other dates. This can be explained by the long groundwater draining period associated with the drying stage, during which no river water enters the aquifer.

While previous studies have shown that mixing between the river and the groundwater mostly explains the decrease in aquifer NO$_3^-$ concentrations (Pinay et al., 1998; Baillieux et al., 2014), others studies have identified different sources leading to the NO$_3^-$ dilution, such as groundwater flowing upwards from the shallow bedrock aquifer (Craig et al., 2010) or from upland terrace recharge (Pfeiffer et al., 2006). In this study, the river–groundwater water exchanges were found to be essential in explaining NO$_3^-$ spatio-temporal patterns observed in the shallow aquifer of the study area, which is mainly controlled by the residence time of the highly loaded groundwater flowing from the agricultural area to the river. Temporal variations in the degree of mixing can also be observed and are controlled by the hydrological cycle, especially drying stage duration and flood occurrences.

The second component of the PLSR (14% of NO_3^- variance explained) is mainly related to DOC and alkalinity (negative contribution) and DO and pH (positive contribution). In riverine systems, river water infiltrating through the hyporheic zone can provide groundwater with DO (Boulton et al., 1998; Zarnetske et al., 2012). However, in the study area, the lower DO concentration areas are located along the river channel and therefore these low DO concentrations can more likely be linked to microbial activity consuming oxygen brought by the river water entering the hyporheic zone (Mermillod-Blondin et al., 2005). Alkalinity is a parameter that can be generated in riparian areas through OC oxidation (Vidon et al., 2010) and denitrification (Li and Irvin, 2007). In addition, DOC is a key element for heterotrophic microbial growth and can be linked to heterotrophic activity. DOC is known to be related to heterotrophic activity (Wetzel, 1992), as well as relatively low pH that may be an indicator of high respiration level (Henze, 1997). The results could indicate that nitrate concentrations are affected by a biological process denoted by component 2 of the PLSR and, interacting with pH, fuelled by OC, consuming oxygen and producing alkalinity. Among all the biological processes affecting nitrate, this combination of parameters could be related to denitrification. Indeed, denitrification leads to nitrate removal under anaerobic conditions and uses OC as an electron donor (Rivett et al., 2008) and has been related to alkalinity production (Li and Irvin, 2007). Nitrification occurs in riparian areas, but in this study it was difficult to link component 2 with nitrification, since groundwater in the study area exhibited low ammonium concentrations. Another process that could be considered is the assimilation of nitrate into microbial biomass, but this process can only remove a small amount of nitrate and the rapid bacterial die-off may lead to N release as ammonium and then nitrate in groundwater (Rivett et al., 2008). In addition the probability that component 2 is linked to denitrification is accentuated by the fact that riparian areas are known to be places where high denitrification rates are found (Pinay and Decamps, 1988; Hill et al., 2000; Ranalli and Macalady, 2010) and this has already been observed at the study site (Sánchez-Pérez et al., 2003; Iribar et al., 2008). Denitrification had a lower impact on NO_3^- concentrations than water mixing, but unlike mixing denitrification leads to effective N removal from the groundwater (Pinay et al., 1998).

4.2. Environmental factors controlling DEA

In this study, DEA was used as an indicator of denitrification under optimal and standardised carbon and nitrate supply. While
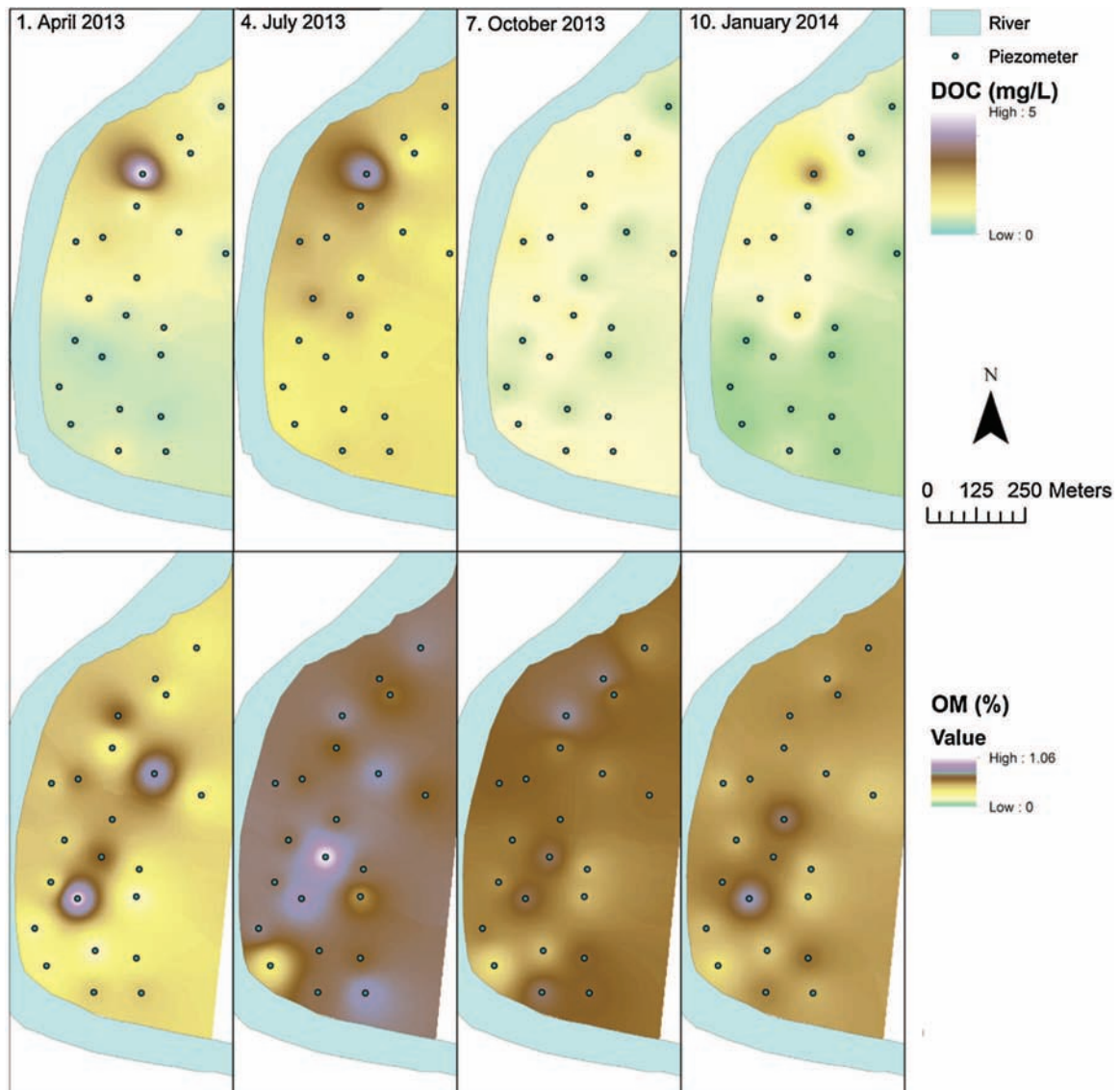

Fig. 6. Maps of interpolated (IDW) DOC (top) and OM (bottom) for the four full campaigns.
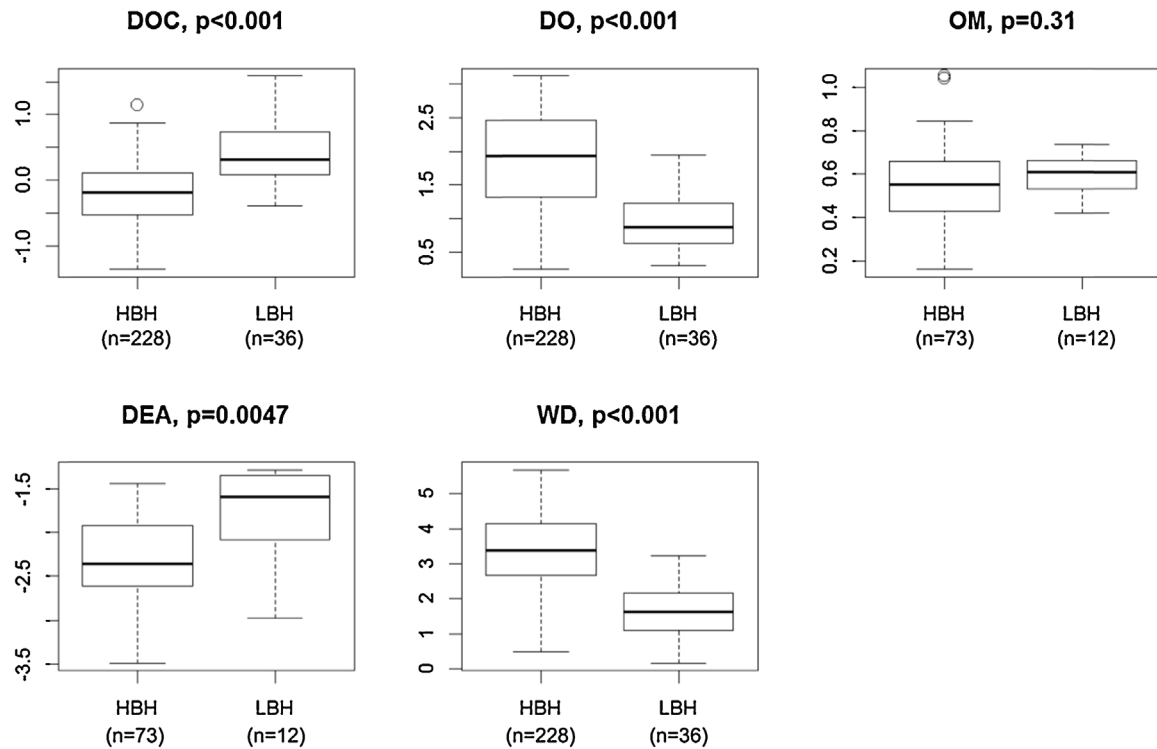
Fig. 7. Boxplot of DOC, DO, OM, DEA and WD according to the two bank geomorphology types (LBH and HBH). DOC, DEA and DO were transformed to ensure normality of the data distribution. *p*-Values are calculated with Student *t*-test.

DEA measures the potential capacity of denitrifying communities under optimal conditions and does not represent actual *in situ* rate of denitrification, it has been related to the functional response (denitrification) of denitrifying communities (Iribar et al., 2008). DEA measured in the study area varied over several orders of magnitude. The average rate was $0.022 \, \mu$g-N g-sed^{-1} h^{-1}, which is consistent with the rates reported by Peterson et al. (2013) for subsoil ($0.015 \, \mu$g-N g-sed^{-1} h^{-1}) and slightly higher than the rates they measured in deeper gravel layer ($0.005 \, \mu$g-N g-sed^{-1} h^{-1}) of an alluvial floodplain. However, the highest rate recorded in the area ($0.18 \, \mu$g-N g-sed^{-1} h^{-1}) was lower than the rates measured in topsoil by Miller et al. (2008), which reached $1.3 \, \mu$g-N g-sed^{-1} h^{-1}. Furthermore, the results show that DEA rates in the study area could be very low ($2.2 \times 10^{-4} \, \mu$g-N g-sed^{-1} h^{-1}).

In the present study, high DEA was related to high DOC concentration and OM content and to low DO concentrations, these factors explaining 31% of DEA variance over the study area. OM content has been linked to bacterial density and can be considered a good proxy for bacterial biomass in sediment (Iribar, 2007). Therefore, the occurrence at the same spot of anoxia and high OM could indicate important bacterial activity. The above relationship can thus be explained by the fact that increased heterotrophic bacterial activity in the presence of DOC leads to anoxia (Arango et al., 2007) and growth of bacterial biomass (increasing OM), promoting conditions for denitrification to occur. In addition to being an indicator of bacterial biomass, OM can indicate patches located within sediment and can be a source of OC fuelling the denitrification process (Hill et al., 2000). Therefore, OC dynamics can be interpreted as a key factor explaining spatio-temporal variations in DEA and OC sources need to be thoroughly investigated. Indeed carbon supply is often considered as the major limiting factor for denitrification (Starr and Gillham, 1993; Jacinthe et al., 1998; Devito et al., 2000; Rivett et al., 2008; Zarnetske et al., 2011; Peter et al., 2012). However, bacterial richness, which was the only variable describing the bacterial community, was not related to DEA in this study. The total

DEA variance explained by the others variables was relatively low. Others descriptors such as carbon bioavailability (Baker et al., 2000) or a better descriptor of bacterial communities (Iribar et al., 2008) could have improve explained DEA variance.

OC in alluvial aquifer can originate from two sources: (i) degradation of the OM contained in the sediment and (ii) transported by water flows (Zarnetske et al., 2012). The first source includes the degradation of OM contained in the topsoil layer during high groundwater periods or leaching from leaf litter during inundation (Baldwin and Mitchell, 2000). Isolated OM patches such as buried channel deposits can also provide a source of OC within sediments (Hill et al., 2000). OC can also be related to the DOC brought by the river through lateral recharge and overbank flow infiltration during flood events (Peyrard et al., 2011; Zarnetske et al., 2012). The role of DOC coming from the river in the study area has been reported previously (Sánchez-Pérez et al., 2003), but recent modelling studies show that DOC input in the riparian area through the river plays a small role in comparison with the *in situ* sediment particulate organic carbon (POC) content (Sun, 2015). In this study DOC concentrations were higher near the river and in the period following a flood and can be linked to river transport. However, the DOC concentrations are not related to conservative tracers such as Cl$^-$, suggesting that the DOC can also originate from another source, such as sediment OM dissolution.

Differences in DEA and related factors were investigated for two different types of bank geomorphology, LBH and HBH. DEA, in relation to DOC and DO, was more important in LBH than in HBH areas, making the LBH areas DEA hotspots. Geomorphology is known to affect denitrification in riparian areas (Gold et al., 2001; Vidon and Hill, 2004; Ranalli and Macalady, 2010). Hill (1996) indicated that denitrification is promoted in riparian areas with an impermeable layer close to the surface forcing the groundwater to flow into areas where conditions are optimum for denitrification. This setting corresponds to the LBH areas of this study. The lower water table, increasing the contact between water and topsoil layer containing a
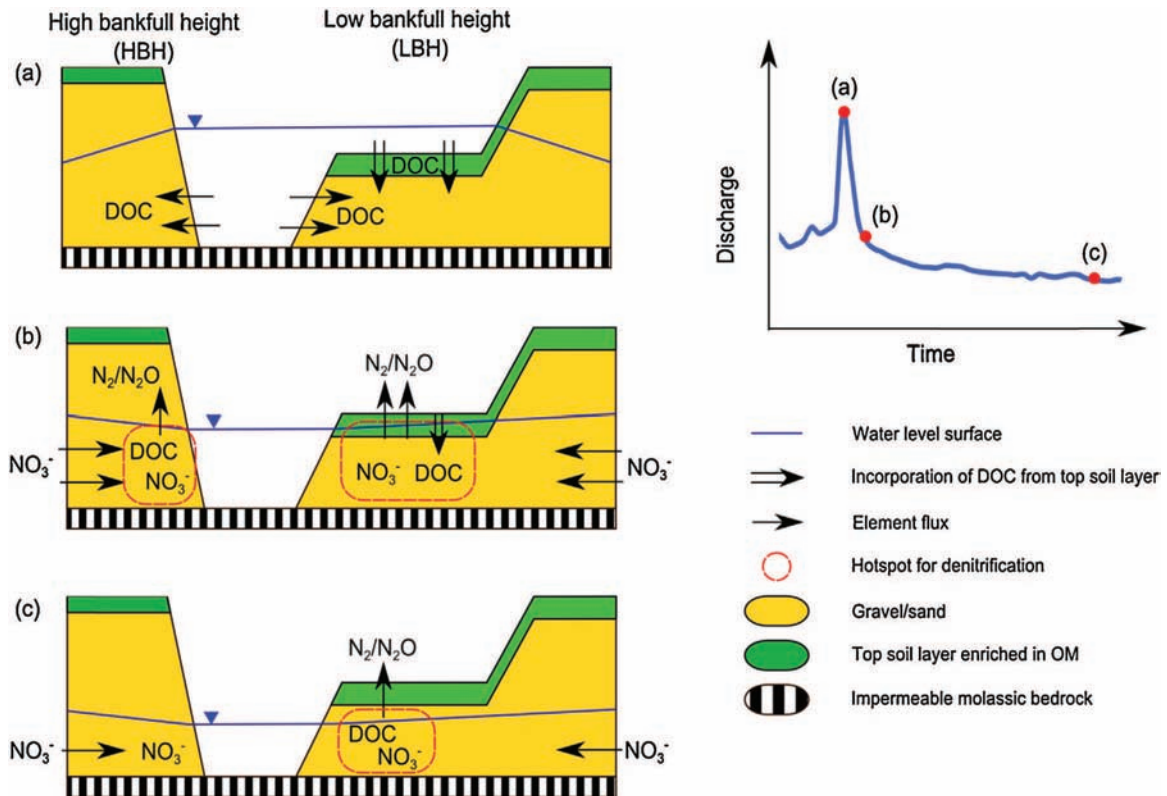
Fig. 8. Conceptual diagram of denitrification process in the floodplain. High bankfull height (HBF) corresponds to the left bank and low bankfull height (LBF) to the right bank in the diagram. (a) During the flood, DOC enters the aquifer with river water and is degraded from OM of the topsoil layer; (b) after the flood, denitrification hotspots occur in HBF and LBF; (c) after a long drying stage, denitrification is lower and only occurs in LBF.

high OM content, may explain the high DEA measured in LBH areas. In addition the OM content was not different between the two types of geomorphology and some high values found were related to DEA hotspots located outside the LBH area.

4.3. Conceptual model of denitrification in alluvial floodplains

Analysis of the spatio-temporal variations in denitrification at the study site allowed a conceptual diagram of denitrification occurrence in alluvial floodplains to be shaped (Fig. 8). The two geomorphological configurations of the banks (LBH and HBH) showed differences in denitrification processes. To explain the dynamics of denitrification and nitrate in a floodplain, a typical temporal sequence starting from a flood event to the end of the drying stage has to be taken into consideration. During flooding, DOC coming from the river flow enters the aquifer through bank recharge in HBH and LBH. In addition, OC from the topsoil layer is incorporated into the groundwater in LBH, where the groundwater level reaches the surface and through leaching due to the infiltration of over-bank flow (Fig. 8a). There is consequently more DOC in LBH due to its dual origin than in HBH. Then, following the flood, denitrification occurs at a significant rate in HBH and LBH, and nitrate flowing from the agricultural area to the river is consumed at both locations (Fig. 8b). After a drying period, the duration of which depends on the river floodplain geomorphological settings, DOC is entirely consumed in HBH and no longer supports denitrification. However, DOC concentrations are higher in LBH than in HBH after the flood and the groundwater remains close to the surface for a longer period, making OC in the soil still available in LBH. Therefore, in LBH, denitrification remains active for a longer period during the drying stage (Fig. 8c). Denitrification in LBH decreases as the drying stage continues and eventually ceases.

Some local deviations from the generalised nitrate dynamics described above were observed in the data and may be due to local heterogeneity of the substrate affecting flow paths or local OM content. However, these observations were rather rare in view of the high density of sampling points, indicating that significant conclusions can be drawn from this study. This work was based on the hypothesis that denitrification is the most important process of nitrate removal, but the shallow water table in LBH areas would allow plant uptake to occur (Pinay et al., 1998). This process would result in greater nitrate removal rates and should be included in further studies for better evaluation of nitrate removal potential of the riparian area.

5. Conclusions

This study examined the characteristics of processes occurring in a floodplain area, with the focus on denitrification patterns and nitrate dynamics. PLSR analysis revealed that NO_3^- concentrations in groundwater were mainly controlled by the mixing between river water and groundwater and denitrification also played a significant role in nitrate removal. Potential denitrification rates were strongly linked to the presence of DOC, OM and anoxia. However, many factors, including geomorphology and hydrological cycle, appeared to control potential denitrification hot spot and hot moment patterns. The combination of these factors led to complex and heterogeneous nitrate dynamics in the study area. These findings show that accurate assessments of denitrification rates and nitrate loads in floodplain environments from field studies can be made from detailed datasets. Due to the difficulty of getting a complete field dataset for every location, modelling work integrating all these factors might be a valuable tool in evaluating floodplain

nitrate mitigation potential under different floodplain configurations.

Acknowledgments

References

Abdi, H., 2010. Partial least squares regression and projection on latent structure regression (PLS Regression). Wiley Interdisc. Rev. Comput. Stat. 2, 97–106.

Amoros, C., Bornette, G., Cedex, V., 2002. Connectivity and biocomplexity in waterbodies of riverine floodplains. Freshw. Biol. 47, 761–776, http://dx.doi.org/10.1046/j.1365-2427.2002.00905.x.

Arango, C.P., Tank, J.L., Schaller, J.L., Royer, T.V., Bernot, M.J., David, M.B., 2007. Benthic organic carbon influences denitrification in streams with high nitrate concentration. Freshw. Biol. 52, 1210–1222.

Arauzo, M., Valladolid, M., Martínez-Bastida, J.J., 2011. Spatio-temporal dynamics of nitrogen in river-alluvial aquifer systems affected by diffuse pollution from agricultural sources: implications for the implementation of the Nitrates Directive. J. Hydrol. 411, 155–168, http://dx.doi.org/10.1016/j.jhydrol.2011.10.004.

Arrate, I., Sanchez-Perez, J.-M., Antiguedad, I., Vallecillo, M.A., Iribar, V., Ruiz, M., 1997. Groundwater pollution in Quaternary aquifer of Vitoria–Gasteiz (Basque Country, Spain). Environ. Geol. 30, 257–265.

Baillieux, A., Campisi, D., Jammet, N., Bucher, S., Hunkeler, D., 2014. Regional water quality patterns in an alluvial aquifer: direct and indirect influences of rivers. J. Contam. Hydrol. 169, 123–131, http://dx.doi.org/10.1016/j.jconhyd.2014.09.002.

Baker, M.A., Valett, H.M., Dahm, C.N., 2000. Organic carbon supply and metabolism in a shallow groundwater ecosystem. Ecology 81, 3133–3148.

Baker, M.A., Vervier, P., 2004. Hydrological variability, organic matter supply and denitrification in the Garonne River ecosystem. Freshw. Biol. 49, 181–190, http://dx.doi.org/10.1046/j.1365-2426.2003.01175.x.

Baldwin, D.S., Mitchell, A.M., 2000. The effects of drying and re-flooding on the sediment and soil nutrient dynamics of lowland river–floodplain systems: a synthesis. Regul. Rivers Res. Manage. 16, 457–467, doi:10.1002/1099-1646(200009/10)16:5<457::AID-RRR597>3.0.CO;2-B.

Bijay-Singh, Yadvinder-Singh, Sekhon, G.S., 1995. Fertilizer-N use efficiency and nitrate pollution of groundwater in developing countries. J. Contam. Hydrol. 20, 167–184, http://dx.doi.org/10.1016/0169-7722(95)00067-4.

Böhlke, J.-K., 2002. Groundwater recharge and agricultural contamination. Hydrogeol. J. 10, 153–179.

Boulton, A.J., Findlay, S., Marmonier, P., Stanley, E.H., Valett, H.M., 1998. The functional significance of the hyporheic zone in streams and rivers. Annu. Rev. Ecol. Syst. 29, 59–81, http://dx.doi.org/10.1146/annurev.ecolsys.29.1.59.

Burt, T.P., Matchett, L.S., Goulding, K.W.T., Webster, C.P., Haycock, N.E., 1999. Denitrification in riparian buffer zones: the role of floodplain hydrology. Hydrol. Processes 13, 1451–1463, doi:10.1002/(SICI)1099-1085(199907)13:10<1451::AID-HYP822>3.0.CO;2-W.

Carpenter, S.R., Caraco, N.F., Correll, D.L., Howarth, R.W., Sharpley, A.N., Smith, V.H., 1998. Non point pollution of surface waters with phosphorus and nitrogen. Ecol. Appl. 8, 559–568, doi:10.1890/1051-0761(1998)008[0559:NPOSWW]2.0.CO;2.

Carrascal, L.M., Galván, I., Gordo, O., 2009. Partial least squares regression as an alternative to current regression methods used in ecology. Oikos 118, 681–690, http://dx.doi.org/10.1111/j.1600-0706.2008.16881.x.

Craig, L., Bahr, J.M., Roden, E.E., 2010. Localized zones of denitrification in a floodplain aquifer in southern Wisconsin, USA. Hydrogeol. J. 18, 1867–1879.

Devito, K.J., Fitzgerald, D., Hill, A.R., Aravena, R., 2000. Nitrate dynamics in relation to lithology and hydrologic flow path in a river riparian zone. J. Environ. Qual. 29, 1075–1084.

Dosskey, M.G., Vidon, P., Gurwick, N.P., Allan, C.J., Duval, T.P., Lowrance, R., 2010. The role of riparian vegetation in protecting and improving chemical water quality in streams. JAWRA J. Am. Water Resources Assoc. 46, 261–277, http://dx.doi.org/10.1111/j.1752-1688.2010.00419.x.

Epstein, S., Mayeda, T., 1953. Variation of O 18 content of waters from natural sources. Geochim. Cosmochim. Acta 4, 213–224.

ESRI, R., 2011. ArcGIS Desktop: Release 10. Environmental Systems Research Institute, CA.

Gold, A.J., Groffman, P.M., Addy, K., Kellogg, D.Q., Stolt, M., Rosenblatt, A.E., 2001. Landscape Attributes as Controls on Groithd Water Nitrate Removal Capacity of Riparian Zones.

Gonfiantini, R., 1978. Standards for Stable Isotope Measurements in Natural Compounds.

Groffman, P., Butterbach-Bahl, K., Fulweiler, R., Gold, A., Morse, J., Stander, E., Tague, C., Tonitto, C., Vidon, P., 2009. Challenges to incorporating spatially and temporally explicit phenomena (hotspots and hot moments) in denitrification models. Biogeochemistry 93, 49–77, http://dx.doi.org/10.1007/s10533-008-9277-5.

Henze, M., 1997. Basic biological processes. In: Wastewater Treatment. Springer, pp. 55–112.

Hill, A.R., 1996. Nitrate removal in stream riparian zones. J. Environ. Qual. 25, 743–755.

Hill, A.R., Devito, K.J., Campagnolo, S., Sanmugadas, K., 2000. Subsurface denitrification in a forest riparian zone: interactions between hydrology and supplies of nitrate and organic carbon. Biogeochemistry 51, 193–223.

Iribar, A., 2007. Composition des communautés bactériennes dénitrifiantes au sein d'un aquifère alluvial et facteurs contrôlant leur structuration: relation entre structure des communautés et dénitrification. Université de Toulouse III – Paul Sabatier.

Iribar, A., Sánchez-Pérez, J., Lyautey, E., Garabétian, F., 2008. Differentiated free-living and sediment-attached bacterial community structure inside and outside denitrification hotspots in the river–groundwater interface. Hydrobiologia 598, 109–121, http://dx.doi.org/10.1007/s10750-007-9143-9, LA – English.

Jacinthe, P.-A., Groffman, P.M., Gold, A.J., Mosier, A., 1998. Patchiness in microbial nitrogen transformations in groundwater in a riparian forest. J. Environ. Qual. 27, 156–164.

Jégo, G., Sánchez-Pérez, J.M., Justes, E., 2012. Predicting soil water and mineral nitrogen contents with the STICS model for estimating nitrate leaching under agricultural fields. Agric. Water Manage. 107, 54–65, http://dx.doi.org/10.1016/j.agwat.2012.01.007.

Kendall, C., McDonnell, J.J., 2012. Isotope Tracers in Catchment Hydrology. Elsevier.

Korom, S.F., 1992. Natural denitrification in the saturated zone: a review. Water Resources Res. 28, 1657–1668, http://dx.doi.org/10.1029/92WR00252.

Lamontagne, S., Herczeg, A.L., Dighton, J.C., Jiwan, J.S., Pritchard, J.L., 2005. Patterns in groundwater nitrogen concentration in the floodplain of a subtropical stream (Wollombi Brook, New South Wales). Biogeochemistry 72, 169–190, http://dx.doi.org/10.1007/s10533-004-0358-9.

Li, B., Irvin, S., 2007. The comparison of alkalinity and ORP as indicators for nitrification and denitrification in a sequencing batch reactor (SBR). Biochem. Eng. J. 34, 248–255, http://dx.doi.org/10.1016/j.bej.2006.12.020.

McClain, M.E., Boyer, E.W., Dent, C.L., Gergel, S.E., Grimm, N.B., Groffman, P.M., Hart, S.C., Harvey, J.W., Johnston, C.A., Mayorga, E., McDowell, W.H., Pinay, G., 2003. Biogeochemical hot spots and hot moments at the interface of terrestrial and aquatic ecosystems. Ecosystems 6, 301–312, http://dx.doi.org/10.1007/s10021-003-0161-9.

Mermillod-Blondin, F., Mauclaire, L., Montuelle, B., 2005. Use of slow filtration columns to assess oxygen respiration, consumption of dissolved organic carbon, nitrogen transformations, and microbial parameters in hyporheic sediments. Water Res. 39, 1687–1698, http://dx.doi.org/10.1016/j.watres.2005.02.003.

Mevik, B.-H., Wehrens, R., 2007. The pls package: principal component and partial least squares regression in R. J. Stat. Softw. 18, 1–24.

Miller, M.N., Zebarth, B.J., Dandie, C.E., Burton, D.L., Goyer, C., Trevors, J.T., 2008. Crop residue influence on denitrification, N_2O emissions and denitrifier community abundance in soil. Soil Biol. Biochem. 40, 2553–2562, http://dx.doi.org/10.1016/j.soilbio.2008.06.024.

Naiman, R.J., Decamps, H., McClain, M.E., 2010. Riparia: Ecology, Conservation, and Management of Streamside Communities. Academic Press.

Peter, S., Rechsteiner, R., Lehmann, M.F., Tockner, K., Durisch-Kaiser, E., 2011. Denitrification Hot Spot and Hot Moments in a Restored Riparian System. IAHS-AISH Publication, pp. 433–436.

Peter, S., Rechsteiner, R., Lehmann, M.F., Brankatschk, R., Vogt, T., Diem, S., Wehrli, B., Tockner, K., Durisch-Kaiser, E., 2012. Nitrate removal in a restored riparian groundwater system: functioning and importance of individual riparian zones. Biogeosci. Discuss. 9, 6715–6750.

Peterson, M.E., Curtin, D., Thomas, S., Clough, T.J., Meenken, E.D., 2013. Denitrification in vadose zone material amended with dissolved organic matter from topsoil and subsoil. Soil Biol. Biochem. 61, 96–104, http://dx.doi.org/10.1016/j.soilbio.2013.02.010.

Peyrard, D., Sauvage, S., Vervier, P., Sánchez-Pérez, J.-M., Quintard, M., 2008. A coupled vertically integrated model to describe lateral exchanges between surface and subsurface in large alluvial floodplains with a fully penetrating river. Hydrol. Processes 22, 4257–4273, http://dx.doi.org/10.1002/hyp.7035.

Peyrard, D., Delmotte, S., Sauvage, S., Namour, P., Gerino, M., Vervier, P., Sánchez-Pérez, J.M., 2011. Longitudinal transformation of nitrogen and carbon in the hyporheic zone of an N-rich stream: a combined modelling and field study. Phys. Chem. Earth A/B/C 36, 599–611, http://dx.doi.org/10.1016/j.pce.2011.05.003.

Pfeiffer, S.M., Bahr, J.M., Beilfuss, R.D., 2006. Identification of groundwater flow-paths and denitrification zones in a dynamic floodplain aquifer. J. Hydrol. 325, 262–472, http://dx.doi.org/10.1016/j.jhydrol.2005.10.019.

Pinay, G., Decamps, H., 1988. The role of riparian woods in regulating nitrogen fluxes between the alluvial aquifer and surface water: a conceptual model. Regul. Rivers 2, 507–516.

Pinay, G., Ruffinoni, C., Wondzell, S., Gazelle, F., 1998. Change in groundwater nitrate concentration in a large river floodplain: denitrification, uptake, or mixing? J. N. Am. Benthol. Soc. 17, 179–189, http://dx.doi.org/10.2307/1467961.

Power, J.F., Schepers, J.S., 1989. Nitrate contamination of groundwater in North America. Agric. Ecosyst. Environ. 26, 165–187, http://dx.doi.org/10.1016/0167-8809(89)90012-1.

R Core Team, 2012. R: A Language and Environment for Statistical Computing. R Foundation for Statistical Computing, Vienna, Austria.

Ranalli, A.J., Macalady, D.L., 2010. The importance of the riparian zone and in-stream processes in nitrate attenuation in undisturbed and agricultural watersheds – a review of the scientific literature. J. Hydrol. 389, 406–415, http://dx.doi.org/10.1016/j.jhydrol.2010.05.045.

Rivett, M.O., Buss, S.R., Morgan, P., Smith, J.W.N., Bemment, C.D., 2008. Nitrate attenuation in groundwater: a review of biogeochemical controlling processes. Water Res. 42, 4215–4232, http://dx.doi.org/10.1016/j.watres.2008.07.020.

Sánchez-Pérez, J.M., Tremolieres, M., Carbiener, R., 1991a. Une station d'épuration naturelle des phosphates et nitrates apportés par les eaux de débordement du Rhin: la forêt alluviale à frêne et orme. C. R. Acad. Sci. Sér. 3, Sci. Vie 312, 395–402.

Sánchez-Pérez, J.M., Tremolieres, M., Schnitzler, A., Carbiener, R., 1991b. Evolution de la qualité physico-chimique des eaux de la frange superficielle de la nappe phréatique en fonction du cycle saisonnier et des stades de succession des forêts alluviales rhénanes (Querco-Ulmetum minoris Issl. 24). Acta Oecol. (1990) 12, 581–601.

Sánchez-Pérez, J.M., Vervier, P., Garabétian, F., Sauvage, S., Loubet, M., Rols, J.L., Bariac, T., Weng, P., 2003. Nitrogen dynamics in the shallow groundwater of a riparian wetland zone of the Garonne, SW France: nitrate inputs, bacterial densities, organic matter supply and denitrification measurements. Hydrol. Earth Syst. Sci. 7, 97–107, http://dx.doi.org/10.5194/hess-7-97-2003.

Seitzinger, S., Harrison, J.A., Böhlke, J.K., Bouwman, A.F., Lowrance, R., Peterson, B., Tobias, C., Van Drecht, G., 2006. Denitrification across landscapes and water-scapes: a synthesis. Ecol. Appl. 16, 2064–2090.

Starr, R.C., Gillham, R.W., 1993. Denitrification and organic carbon availability in two aquifers. Groundwater 31, 934–947.

Sun, X., Bernard-Jannin, L., Garneau, C., Volk, M., Arnold, J.G., Srinivasan, R., Sauvage, S., Sánchez-Pérez, J.M., 2015. Improved simulation of river water and ground-water exchange in an alluvial plain using the SWAT model. Hydrol. Processes.

Sun, X., 2015. Modélisation des échanges nappe-rivière et du processus de déni-trification dans les plaines alluviales à l'échelle du bassin versant. Université Toulouse III – Paul Sabatier.

Sutton, M.A., Howard, C.M., Erisman, J.W., Billen, G., Bleeker, A., Grennfelt, P., van Grinsven, H., Grizzetti, B., 2011. The European Nitrogen Assessment: Sources, Effects and Policy Perspectives. Cambridge University Press.

Tockner, K., Stanford, J.A., 2002. Riverine flood plains: present state and future trends. Environ. Conserv. 29, 308–330.

Vidon, P.G.F., Hill, A.R., 2004. Landscape controls on nitrate removal in stream ripar-ian zones. Water Resources Res., 40.

Vidon, P.G., Hill, A.R., 2006. A landscape-based approach to estimate riparian hydro-logical and nitrate removal functions. JAWRA J. Am. Water Resources Assoc. 42, 1099–1112.

Vidon, P., Allan, C., Burns, D., Duval, T.P., Gurwick, N., Inamdar, S., Lowrance, R., Okay, J., Scott, D., Sebestyen, S., 2010. Hot spots and hot moments in ripar-ian zones: potential for improved water quality management. JAWRA J. Am. Water Resources Assoc. 46, 278–298, http://dx.doi.org/10.1111/j.1752-1688.2010.00420.x.

Weiss, R.F., Price, B.A., 1980. Nitrous oxide solubility in water and seawater. Mar. Chem. 8, 347–359, http://dx.doi.org/10.1016/0304-4203(80)90024-9.

Weng, P., Sánchez-Pérez, J.M., Sauvage, S., Vervier, P., Giraud, F., 2003. Assessment of the quantitative and qualitative buffer function of an alluvial wetland: hydro-logical modelling of a large floodplain (Garonne River, France). Hydrol. Processes 17, 2375–2392, http://dx.doi.org/10.1002/hyp.1248.

Wetzel, R.G., 1992. Gradient-dominated ecosystems: sources and regulatory func-tions of dissolved organic matter in freshwater ecosystems. In: Dissolved Organic Matter in Lacustrine Ecosystems. Springer, pp. 181–198.

Yan, B., Fang, N.F., Zhang, P.C., Shi, Z.H., 2013. Impacts of land use change on water-shed streamflow and sediment yield: an assessment using hydrologic modelling and partial least squares regression. J. Hydrol. 484, 26–37, http://dx.doi.org/10.1016/j.jhydrol.2013.01.008.

Zarnetske, J.P., Haggerty, R., Wondzell, S.M., Baker, M.A., 2011. Labile dissolved organic carbon supply limits hyporheic denitrification. J. Geophys. Res. Bio-geosci. (2005–2012), 116.

Zarnetske, J.P., Haggerty, R., Wondzell, S.M., Bokil, V.A., González-Pinzón, R., 2012. Coupled transport and reaction kinetics control the nitrate source-sink function of hyporheic zones. Water Resources Res., 48.

Zhang, W.L., Tian, Z.X., Zhang, N., Li, X.Q., 1996. Nitrate pollution of groundwater in northern China. Agric. Ecosyst. Environ. 59, 223–231, http://dx.doi.org/10.1016/0167-8809(96)01052-3.